Turbidity Study of Spinodal Decomposition of an *N*-Isopropylacrylamide Gel

Yong Li

Kimberly-Clark Corporation, Neenah, Wisconsin 54956

Guonan Wang and Zhibing Hu*

Department of Physics, University of North Texas, Denton, Texas 76203

Received February 15, 1995; Revised Manuscript Received April 3, 1995[⊗]

ABSTRACT: The kinetics of the spinodal decomposition of the volume phase transition of an *N*-isopropylacrylamide gel is studied using a turbidity technique. Three stages were identified: the early stage, the transition stage, and the frozen stage. The early stage can be explained by Cahn–Hilliard–Cook's theory. In the transition stage, the cascading network segment association process causes the turbidity to increase faster than the early stage. The transition stage is characterized by its turbidity growth peak. The final stage, the frozen stage, is characterized by the high turbidity and vanishing turbidity growth rate. In this stage, the spatial concentration variation is frozen and the system enters a semistable state.

I. Introduction

It is known that, when a typical critical phase transition system undergoes a transition from the one-phase state to the two-phase coexistence state along the critical isochore path, spinodal decomposition occurs. The spinodal decomposition process of polymer solution systems can be divided into four stages: the early stage, the intermediate stage, the transition stage, and the later stage.[1] An important parameter characterizing these stages is the concentration fluctuation wavevector q_m. In the early stage, q_m is independent of time but the fluctuation amplitude increases. In the intermediate stage, the wave vector q_m becomes time dependent and starts to shift toward zero. The amplitude continues to increase with time. In the transitional stage, the amplitude reaches the concentrations of two coexistence states and cannot increase any further. Therefore, the transition stage is characterized by the fixed amplitude and a finite interfacial thickness between the two states. In the later stage, the wavevector continuously shifts toward zero, with the interfacial thickness approaching zero.

The volume phase transition of gels can be induced by external stimuli such as temperature, solvent, and electric field.[2–4] It has been shown that the gel volume phase transition is Ising-like.[5] An analogy can be drawn between the gel volume phase transition and the liquid–vapor transition. The gel swollen phase (low polymer concentration) corresponds to the vapor phase, and the gel collapsed phase (high polymer concentration) corresponds to the liquid phase. Although the critical point of the liquid–vapor system can be approached by either an isochore path (constant volume) or an isobar path (constant pressure), the most practical path for the gel system is isobaric. Along the isobaric path, the volume of the sample is measured as a function of external parameters (e.g., temperature, solvent composition, light intensity, etc.). The kinetics of gel volume change involves absorbing/desorbing solvent by the gel network, which is a diffusive process.[5–7] This process is slow, in general, and is even slower near the critical point due to the softening of the network elasticity.[7] This is also supported by the light scattering and kinetic studies of *N*-isopropylacrylamide (NIPA) gels.[4,8] It was found that the collective diffusion coefficient diminishes, and the relaxation time for swelling (or collapsing) diverges by approaching the critical temperature.[4,8]

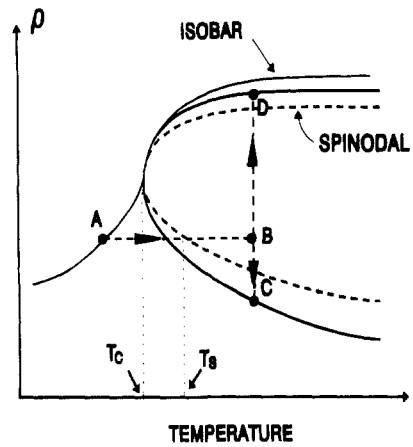

Figure 1. Illustrative phase diagram of an NIPA gel system. As a result of hydrophobic interaction, the coexistence curve (thick solid line) is inverted. The gel network concentration versus temperature is represented using a thin solid line. The spinodal boundary is shown by a dashed line.

The time-resolved light scattering[9,10] has revealed that the early stage spinodal decomposition of the gel volume phase transition is similar to that of a typical polymer solution and can be understood based on Cahn–Hilliard–Cook (CHC) theory.[11] The NIPA gel has an inverted phase diagram as shown in Figure 1. It is swollen at low temperature and collapsed at high temperature. The temperature dependence of its network concentration under zero external osmotic pressure (π), i.e., isobar with $\pi = 0$, is also shown in the figure. The spinodal decomposition of the gel can be induced by quenching the sample from a constant temperature (point A) below the spinodal temperature, T_s, to various temperatures above T_s (point B). Due to the slowness of the volume change of the sample (especially when the sample is larger than several

* To whom the correspondence should be addressed.

[⊗] Abstract published in *Advance ACS Abstracts,* May 15, 1995.

0024-9297/95/2228-4194$09.00/0

millimeters), the interior of the sample is initially under constant volume condition, i.e., the thermodynamic path is an isochore (constant volume). As a result, the system stays inside the unstable zone and starts to decompose into two phases with different network concentrations. This concentration fluctuation can scatter light and reduce the transmission of visible light through the gel. The reduction of the transmission is quantified in terms of the sample turbidity.

The total scattered light I_s is the summation of the scattered light in all directions,

$$I_s(t) = \int_0^{\pi} I_s(q,t)\, 2\pi \sin(\theta)\, d\theta \qquad (1)$$

where θ is the scattering angle, q is the scattering wavevector, and t is time. Since $q = (4\pi n/\lambda)\sin(\theta/2)$, one has

$$I_s(t) = \frac{\lambda^2}{2\pi n^2}\int_0^{q_\pi} I_s(q,t)\, q\, dq \qquad (2)$$

where $q_\pi = 4\pi n/\lambda$ is the wavevector of the back-scattered light, λ is the wavelength, and n is the refractive index. The turbidity A is defined as the light intensity reduction per unit penetration length in the sample, $A = -(1/I)(\delta I/\delta x)$, with I the light intensity in the sample. For a small enough δx, no multiple scattering will occur in δx and the δI is equal to I_s,

$$A = \frac{1}{\delta x}\left(\frac{I_s}{I}\right) \qquad (3)$$

The turbidity, which could involve multiple scattering, is therefore directly related to the scattering function I_s which does not involve multiple scattering.

The transmitted light intensity I_t and the incident intensity I_0 are related by the sample turbidity A and thickness L,

$$I_t/I_0 = e^{-AL} \qquad (4)$$

Therefore, turbidity can be obtained from the ratio of the transmitted light intensity to the incident intensity, $A = -(1/L)\ln(I_t/I_0)$.

The turbidity measurement has been used to study the spinodal decomposition and to measure critical exponents for many systems.[12,13] Most of these systems are in the equilibrium state at varying temperatures. In this paper, we report our result on the kinetics of the gel phase transition.

II. Experimental Section

The NIPA gel samples were made by free-radical polymerization.[14] A mixture of 7.8 g of *N*-isopropylacrylamide (Kodak Co.), 133 mg of methylenebis(acrylamide) as cross-linker, and tetramethylethylenediamine (240 μL) as accelerator, was dissolved in 100 mL of deionized and distilled water. Nitrogen gas was bubbled through the solution to remove dissolved oxygen. Then ammonium persulfate (40 mg) as polymerization initiator was added to the solution. A thin film of the solution was cast between two microslides with a fixed separation of 1 mm. The samples were left untouched for about 12 h before being transferred into a water bath to swell. The swelling ratio measurement was performed and confirmed that the sample underwent the volume phase transition with a transition temperature T_c around 33.8 °C. Since the quenching path in Figure 1 was slightly off the critical point, the spinodal temperature T_s (=34.74 °C), determined by the turbidity method, was higher than T_c.

The absorbance (=log(I_t/I_0)) of gel samples was monitored by a spectrophotometer (Spectronic 301, Milton Roy Ltd.) operating at a wavelength of 555 nm. The conversion from absorbance to turbidity was performed by multiplying the absorbance by a factor of ln(10)/L, where L is the sample thickness, about 1 mm. The temperature of the samples was controlled by a circulation water bath (Brinkmam Lauda Super RM-6) with control accuracy of ±0.05 °C. The temperature at both the sample cell and the circulator was monitored by sensors. In addition, a thermal bath was used to provide the initial temperature of the sample before it was quenched into the two-phase region inside the spectrometer sample holder.

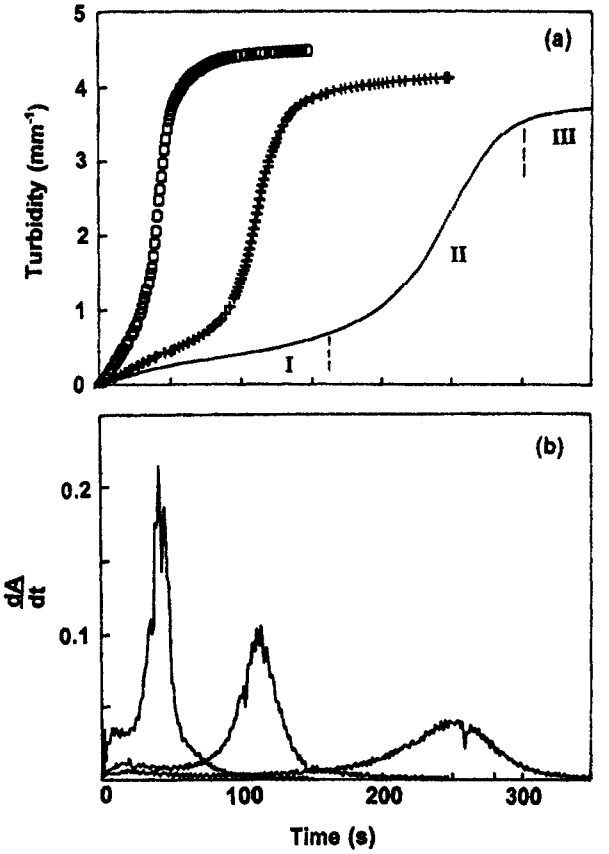

Figure 2. (a) Time-dependent turbidity when the sample was heated up from 32 °C to final temperatures of 35.10 (dot), 35.40 (+), and 36.00 °C (o), respectively. (b) The corresponding derivatives of the turbidity curves. The three regions, I–III, are indicated for the curve with the final temperature equal to 35.1 °C.

III. Results and Discussion

Starting from 32 °C, the sample temperature was raised quickly to various values above T_s by transferring the sample from one water bath to another. The turbidity of the sample is monitored with the time zero point corresponding to the time when the temperature is changed. Parts a and b of Figure 2 show the typical sample turbidity (A) and its growth rate (dA/dt) with final temperatures equal to 35.10, 35.40, and 36.00 °C, respectively. The measurements are reproducible with different samples from the same batch. The development of the turbidity can be divided into three regions. The first one is the slow rise region. The growth rate in this region is represented by the left flat shoulder of the peak in Figure 2b. The second region corresponds to the fast rise of the turbidity, which is the peak area in Figure 2b. The location of the peak corresponds to the time at which the turbidity increased the fastest. The height of the peak is also final temperature dependent: the closer to T_s, the smaller the peak. The turbidity growth rate (and duration) of both regions is related to the final quenching temperature. As can be seen from Figure 2a, the closer the final temperature

is to the critical point, the slower the turbidity kinetics. The third stage (frozen stage) is the turbidity plateau region, where the growth rate is small. It is evident from Figure 2a that the higher the final temperature, the higher the final turbidity value.

A. Early Stage. In the early stage of the spinodal decomposition, the network concentration fluctuations are small. It had been shown be Otake et al. that the scattered light in the early stage of gel spinodal decomposition can be analyzed using CHC theory.[9,10] Specifically, the scattered light intensity I_s is related to the fluctuation growth rate $R(q)$ by[11]

$$I_s(q,t) \sim e^{2R(q)t} \tag{5}$$

with,

$$R(q) = Dq^2\left[1 - \frac{1}{2}\left(\frac{q}{q_m}\right)^2\right] \tag{6}$$

where D is the effective diffusion constant. Using this result and eq 2, the total scattered intensity $I_s(t)$ can be calculated,

$$I_s(t) \sim \frac{1}{y}\int_0^{y_\pi} e^{2D}q_m{}^2 ty(1-y/2)\,dy \tag{7}$$

where $y = (q/q_m)^2$. In the early stage, the concentration fluctuations are mostly associated with individual network segments and are expected to have short correlation length, or large q_m. This means in eq 7 the upper integration limit $y_\pi \ll 1$. From eq 7, the turbidity growth time (τ_1) in the early stage is

$$\tau_1 \sim 1/(Dq_m{}^2) \tag{8}$$

The value of τ_1 is related to the early stage value of $(dA/dt)_0$ by $\tau_1 = (\log e)/(dA/dt)_0$. This early stage is identified by the left shoulder of each of the dA/dt curves in Figure 2b. The fact that these shoulders are flat ($(dA/dt)_0$ = constant) indicates that the time dependence of the turbidity in the early stage is approximately linear. This suggests that the relaxation time τ_1 is much longer than the duration of the early stage. In other words, the onset of the intermediate stage starts before the early stage fluctuation experiences the full exponential growth behavior. This point will become clear later.

The value of q_m can also be related to the correlation length ξ of the concentration fluctuation[8]

$$q_m{}^2 = \frac{1}{2\xi^2} \sim |T - T_c|^{2\nu} \sim |T - T_s|^{2\nu} \tag{9}$$

where ν is a critical exponent. From this relation, the scaling behavior of τ_1 is

$$\tau_1 \sim |T - T_c|^{-(2\nu+x)} \sim |T - T_s|^{-(2\nu+x)} \tag{10}$$

where the exponent x is associated with the scaling behavior of the effective diffusion constant D. Figure 3 is the relaxation turbidity time τ_1 as a function of the reduced temperature ($T - T_s$), with T_s = 34.74 °C. A straight line can be fitted to the data with a slope equal to 1.75. For an Ising system, the value of ν is 0.64. Therefore, the exponent x is equal to 0.47.

Since the turbidity technique is insensitive to the change of q_m, the intermediate stage cannot be identified unambiguously from the early stage.

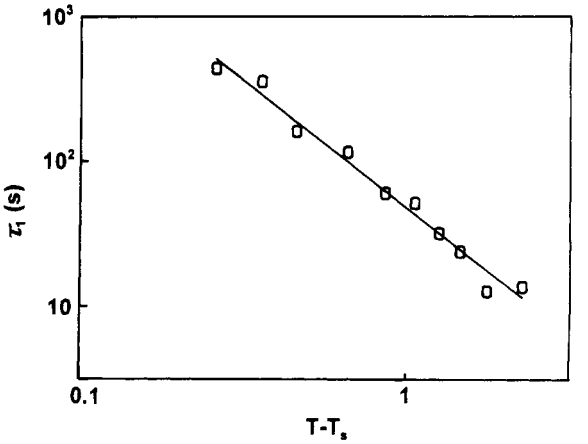

Figure 3. Scaling behavior (log–log plot) of the turbidity rate (τ_1) as a function of reduced temperature. The slope is equal to 1.75.

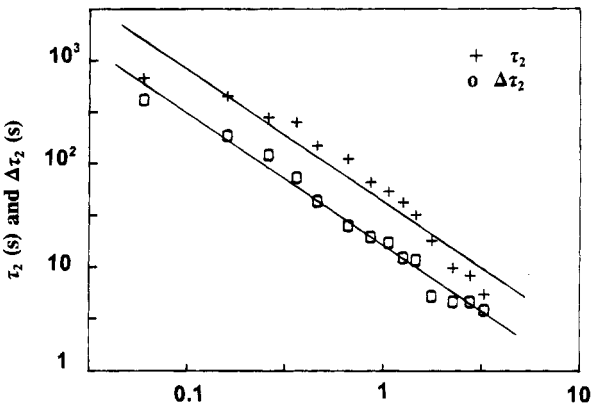

Figure 4. Time τ_2, at which the turbidity derivative reaches its peak value, plotted as a function of final temperature (plus sign). The exponents equal to 1.28. The full width ($\Delta\tau_2$) at half-maximum height of the derivative peak is also plotted (open circles) in the figure. Its slope is equal to 1.28.

B. Transition Stage. Unlike the polymeric systems,[1] the growth rate of the transition stage of the gel system increases and reaches a peak, as shown in Figure 2b. The location of the peak of the turbidity rate is defined as a characteristic time, τ_2, for this stage. τ_2 increases drastically as the temperature approaches T_s. The log–log plot of τ_2 versus the reduced temperature $T - T_s$ is shown in Figure 4 (plus signs). Not only the peak location τ_2 but also the width of the peak $\Delta\tau_2$ has scaling behavior, as shown in the figure (open circles). This indicates that, as the quenching temperature is close to the spinodal temperature, more relaxation modes exist, as expected. As mentioned earlier, the onset of the transition stage ($\tau_2 - \Delta\tau_2$) occurs before the early stage concentration fluctuation experiences exponential growth. This is indicated by the fact that τ_1 is much larger than $\tau_2 - \Delta\tau_2$. The comparison of τ_1, τ_2, and $\Delta\tau_2$ at various temperatures is listed in Table 1.

The increase of turbidity growth rate in the transition stage can be explained with the help of Figure 5. When the gel system is quenched, due to the inherent inhomogeneities in the network structure, some regions have a stronger tendency to collapse than others. Initially, polymer chains aggregate to form bundles in concentrated regions. Since the system is unable to release water quickly, the water content in the nearby dilute regions increases. The further dilution of the already diluted region does not require much energy. Therefore, once some diluted regions are formed, they will be further diluted to facilitate the collapsing of the

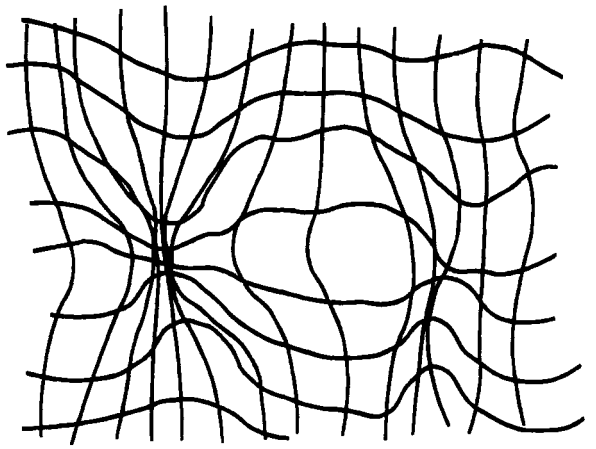

Figure 5. Schematic description of the density fluctuation in the transition stage. The dense region forms stable "filaments".

Table 1. Relaxation times of τ_1, τ_2, and $\Delta\tau_2$ at various temperature $T - T_s$, Where T_s Is Equal to 34.74 °C

$T - T_s$ (°C)	τ_1 (s)	τ_2 (s)	$\Delta\tau_2$ (s)
0.06		677	415
0.16		450	186
0.26	434	280	121
0.36	353	252	72.9
0.46	161	150	43.1
0.66	115	111	25.0
0.86	60.5	65.7	19.5
1.06	51.8	53.6	17.2
1.26	32.2	42.0	12.3
1.46	24.1	31.8	11.6
1.76	12.8	18.0	5.2
2.26	13.7	9.8	4.6
2.76		8.3	4.6
3.26		5.4	3.8

concentrated regions. This cascadelike process is manifested by the peak in the density fluctuation growth.

C. Frozen Stage. As the process of the network chain association continues, the dense regions become denser (point D in Figure 1) and dilute regions become more dilute (beyond point C in Figure 1). Eventually, a stable foamlike structure is formed. This structure is then frozen since the spatial density variation is no longer dynamic. The stability of the structure is balanced by two competing factors: one is the hydrophobic interaction energy among polymer chains, and the other is the bending energy of the aggregated polymer filaments. From the hydrophobic interaction point of view, the system would like to collapse further to minimize exposure to water. However, this would require the filaments to bend, which will cause a high bending energy. As a result, the system adapts the foamlike structure.

D. Comparison with Other Systems. As we have mentioned earlier, there are four stages associated with the spinodal decomposition process of polymer solution systems, as shown in Figure 6a. In comparison, there are also four stages in the gel system (Figure 6b). The intermediate stage in the gel system cannot be identified by the turbidity technique used in this report. The turbidity growth rate is the highest in the early stage in a polymer solution system but is the highest in the transition stage in the gel system. The concentration fluctuations in the polymer system are dynamic throughout the process but frozen (or static) toward the end of the process in the gel system.

In conclusion, the kinetics of the spinodal decomposition near the volume phase transition of NIPA gels has been studied. It is revealed that the kinetics undertakes

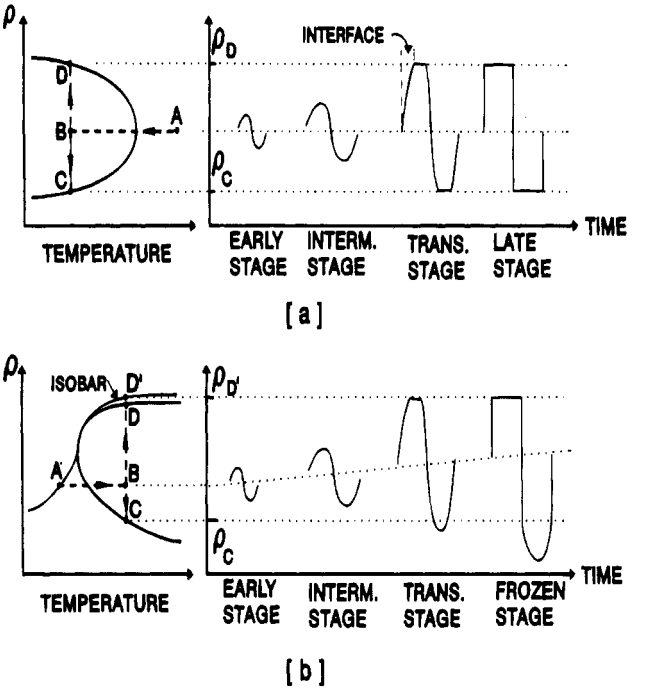

Figure 6. Schematic comparison between the conventional spinodal decomposition process (isochore path) (a) and the gel volume change near the critical point (isobar path) (b). In the former case, the total volume is constant and the system goes from the one-phase state to a two-phase coexistence state. In the latter case, both initial and final states are one-phase states.

three stages: the early stage, the transition stage, and the frozen stage. There may be a possible intermediate stage which cannot be identified using the turbidity technique. The critical slowing down in the early stage has been observed, similar to the Ising systems. In the final stage, the gel is frozen into a foamlike structure, which is different from the final stage of the spinodal decomposition of liquid systems such as polymer solutions and binary liquid systems.

Acknowledgment is made to the donors of the Petroleum Research Fund, administered by the American Chemical Society, and to the U.S. Army Research Office under Grant No. DAAH04-93-G-0215, for support of this research.

References and Notes

(1) Bates, F. S.; Wiltzius, P. *J. Chem. Phys.* **1989**, *91*, 3258.
(2) Li, Y.; Tanaka, T. *Annu. Rev. Mater. Sci.* **1992**, *22*, 243.
(3) Tanaka, T. *ACS Symp Ser.* **1992**, *480*, 1.
(4) Shibayama, M.; Tanaka, T. *Adv. Polym. Sci.* **1993**, *109*, 1.
(5) Li, Y.; Tanaka, T. *J. Chem. Phys.* **1989**, *90*, 5161.
(6) Tanaka, T.; Hocker, L. O.; Benedek, G. B. *J. Chem. Phys.* **1973**, *59*, 5151.
(7) Li, Y.; Tanaka, T. *J. Chem. Phys.* **1990**, *92*, 1365.
(8) Sato-Matsuo, E.; Tanaka, T. *J. Chem. Phys.* **1988**, *89*, 1695.
(9) Otake, K.; Inomata, H.; Yagi, Y.; Konno, M.; Saito, S. *Polym. Commun.* **1989**, *30*, 203.
(10) Inomata, H.; Yagi, Y.; Saito, S. *Macromolecules* **1991**, *24*, 3962.
(11) (a) Cahn, J. W.; Hilliard, J. H. *J. Chem. Phys.* **1958**, *28*, 258. (b) Cook, H. E. *Acta Metall.* **1970**, *18*, 297.
(12) Shen, W.; Smith, G. R.; Knobler, C. M.; Scott, R. L. J. Phys. Chem. **1991**, *95*, 3376.
(13) DaMore, L. W.; Jacobs, D. T. *J. Chem. Phys.* **1992**, *97*, 464.
(14) Hirotsu, S.; Hirokawa, Y.; Tanaka, T. *J. Chem. Phys.* **1987**, *87*, 1392.

MA950199D